

## Complex Impedance Measurements of Acoustical Treatments Used for Underwater Applications:- An Alternative Technique

E J Parker, B V Smith, P Atkins

School of Electronic and Electrical Engineering, The University of Birmingham

### 1. INTRODUCTION

For many years water-loaded impedance tubes and more recently parametric arrays, have been used to measure the acoustic characteristics of underwater acoustical treatments. However, because of their performance limitations and high capital cost there is a requirement for an alternative measurement technique particularly of low impedance treatments in the frequency range 10Hz to 1kHz. Several investigators [1-4] have shown that the complex elastic moduli of a wide range of materials can be determined by affixing accelerometers to each end of a test sample which is excited at one end with a vibration shaker and terminated at the other end with a mass. Acceleration frequency response measurements are then carried out from which the complex moduli can be determined. The technique is equally applicable to the measurement of Young's modulus and shear modulus by the appropriate arrangement of the experiment. This paper reports the preliminary results of an investigation into the development of this technique to enable the measurement of static loading effects upon the measured complex moduli of material samples under test. Providing the sample density is known it is then possible to determine the complex phase speed of the sample from the solution to the wave equation i.e.  $c = \sqrt{\frac{E(1+\eta)}{\rho}}$ . The need for this information when designing acoustical treatments for under water applications is well known, particularly for low impedance spring-like treatments whose acoustical performance is significantly affected by the hydrostatic pressure forces encountered in typical underwater applications. In principle static loads could be applied to a test sample by arranging the experimental setup so that the force of gravity, produced by the terminating end mass, acted on the sample in the appropriate direction. However bearing in mind the hydrostatic loads which are typical this would be quite impractical. It is proposed that the hydrostatic pressure forces may be simulated by mechanically loading the test sample with two compressed air actuators. The test sample is sandwiched between two terminating end masses and the load is applied to the sample as shown in Fig. 1

TEST RIG FOR TESTING SAMPLES UNDER SIMULATED HYDROSTATIC LOAD

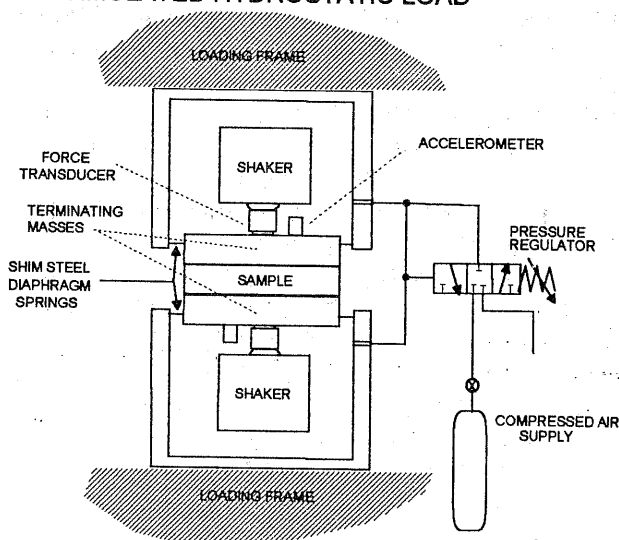


Fig.1

## COMPLEX IMPEDANCE MEASUREMENTS OF ACOUSTICAL TREATMENTS

Air has a relatively low characteristic impedance up to quite high pressures and it will be shown that what effect it has can be completely eliminated from any sample measurements over a useful frequency range. It should also be relatively easy to control the magnitude of the applied load with the appropriate readily available pneumatic circuitry.

The theory used to determine the material properties from the frequency response measurements depends largely upon the frequency range of interest and the properties of the material being tested. At low frequencies and for spring-like specimens a lumped parameter approach is sufficiently accurate and the frequency response matrix can be easily 'inverted' to determine the elastic moduli of the sample as a function of frequency. At high frequencies and for samples which cannot be treated as being spring-like, a wave equation model becomes necessary. Unfortunately this involves the solution of transcendental equations which is not as straight forward. Several investigators e.g. [3,4] have shown that these can be easily solved at resonant frequencies. Unfortunately this only provides moduli measurements at these frequencies rather than as a continuous function of frequency which is yielded by the lumped parameter model. However a method to solve the transcendental equations at narrow frequency intervals has been put forward by Buchanan[5] which involves a numerical solution. It is planned to investigate this technique to determine the complex phase speed of samples at higher frequencies where the lumped parameter model becomes inaccurate. However this paper is confined to the 'inversion' of the response matrix to determine the complex phase speed using a lumped parameter model. Using a multilayer wave equation model to predict the response matrix with known material properties presents no problems however. These results are presented to indicate the frequency range over which the lumped parameter model is sufficiently accurate. Validated complex phase speed measurement results for a high air fraction low density foam sample at atmospheric pressure are presented to demonstrate this. At the time of writing experimental results for a sample under load are not available. However, it will be shown theoretically, using a multilayer wave model to produce the response matrix and a lumped parameter for the inversion of the response matrix, the feasibility of determining complex phase speed for typical low impedance materials at typical hydrostatic pressure loads in the frequency range 10Hz- 1kHz.

## 2. THEORY

### 2.1 Multilayer One Dimensional Wave Equation Model

Figure 2 overleaf is a schematic of the multilayer model of the proposed experimental test rig shown in Figure 1. For a sinusoidal input force stimulus  $F_2$  under steady state conditions the acceleration of the aluminium terminating end masses are  $\ddot{x}_2$  and  $\ddot{x}_5$  respectively. The complex ratio  $\ddot{x}_2/F_2$  corresponds to the point inertance frequency response at boundary 2 and  $\ddot{x}_5/F_2$  the transfer inertance frequency response between boundaries 2 and 5.

If Boundary (n) separates mediums (n) and (n+1), the incident and reflected wave amplitudes at boundary (n) are  $A'(n)$  and  $B(n)$  respectively. The transmitted wave at boundary (n) is  $A(n+1)$ . For brevity, the solution of the wave equation and the derivation of the subsequent expressions used for the analysis of multilayer systems will for the purposes of this paper be omitted. There

## COMPLEX IMPEDANCE MEASUREMENTS OF ACOUSTICAL TREATMENTS

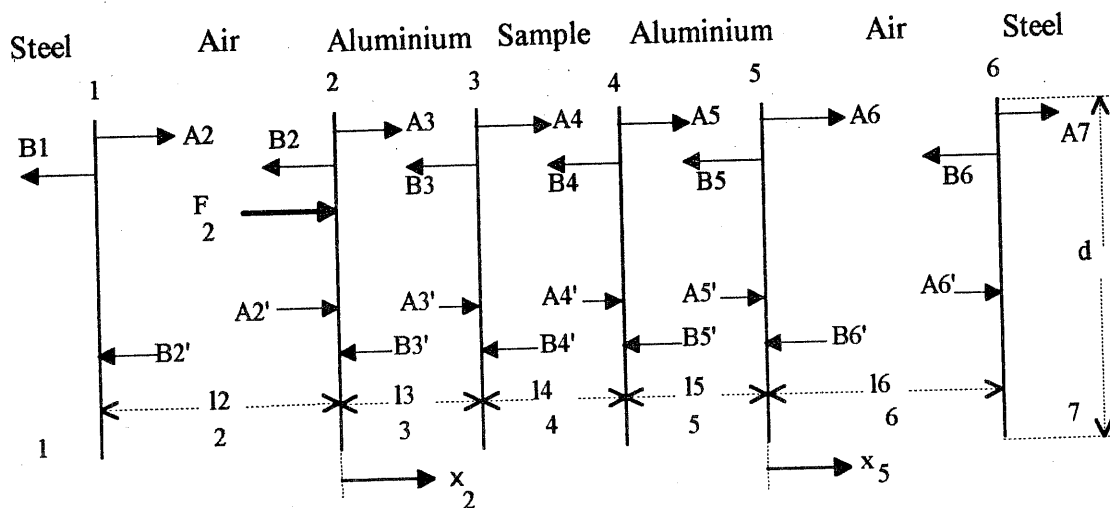


Fig.2

is a wide range of literature which has been published on the subject e.g. [6,7] and the reader should refer to these for further information. It is first of all necessary to determine the specific input impedance at each boundary. This is done using the following expressions.

$$Z_{in_n} = z_{n+1} [Z_{in_{n+1}} + jz_{n+1} \tan k_{n+1} l_{n+1}] / [z_{n+1} + jZ_{in_{n+1}} \tan k_{n+1} l_{n+1}]$$

where  $Z_{in_n}$  = specific input impedance at boundary n looking in direction of layer n+1

$Z_{in_{n+1}}$  = specific input impedance at boundary n+1 looking in direction of layer n+2

$z_{n+1} = \rho_{n+1} c_{n+1}$  where  $\rho_{n+1}$  = density of layer n+1

$c_{n+1}$  = complex phase speed of layer n+1

$k_{n+1}$  = complex wavenumber in layer n+1

$l_{n+1}$  = thickness of layer n+1

Similarly the specific input impedance at boundary n looking in the direction of layer n,

$$Z_{in-n} = z_n [Z_{in_{n-1}} + jz_n \tan k_n l_n] / [z_n + jZ_{in_{n-1}} \tan k_n l_n]$$

Successive applications of these expressions enables the combined input impedance at boundary 2,  $Z_{in_2} + Z_{in-2}$ , to be found. It should be noted that when this is done the starting value for  $Z_{in_6}$  is equal to  $\rho_7 c_7$  and the starting value for  $Z_{in-1}$  is equal to  $\rho_1 c_1$ .

The point inductance at boundary 2 allowing for layer area,  $\dot{x}_2/F_2$ , is then given by,

$$\dot{x}_2/F_2 = j\omega / [(Z_{in_2} + Z_{in-2})\pi d^2/4]$$

The transfer inductance,  $\dot{x}_5/F_2$  is found as follows:-

$$\text{Now } Z_{in_5} = (A'_5 + B_5)/\dot{x}_5$$

where  $\dot{x}_5$  = velocity of boundary 5

$$\text{and } R_5 = B_5/A'_5$$

where  $R_5$  = reflection coefficient at boundary 5

$$= (Z_{in_5} - z_5)/(Z_{in_5} + z_5)$$

$$\text{Rearranging gives } \dot{x}_5 = A'_5(1 + R_5)/Z_{in_5} \quad (1)$$

## COMPLEX IMPEDANCE MEASUREMENTS OF ACOUSTICAL TREATMENTS

Now  $T_{23} = e^{-jk_3 l_3} [Z_{in3} + z_4] / [Z_{in3} + z_3]$

where  $T_{23} = A_4/A_3$  = transmission coefficient from boundary 2 to boundary 3

also  $T_{34} = e^{-jk_4 l_4} [Z_{in4} + z_5] / [Z_{in4} + z_4]$

where  $T_{34} = A_5/A_4$  = transmission coefficient from boundary 3 to boundary 4

Therefore  $A_5 = T_{23} T_{34} A_3$

Now  $A'_5 = e^{-jk_5 l_5} A_5$

substituting into equation (1) gives

$$\dot{x}_5 = T_{23} T_{34} e^{-jk_5 l_5} (1 + R_5) A_3 / Z_{in5}$$

Now it can be shown that

$$A_3 = F_2 [Z_{in2} + z_3] / 2 [Z_{in2} + Z_{in-2}]$$

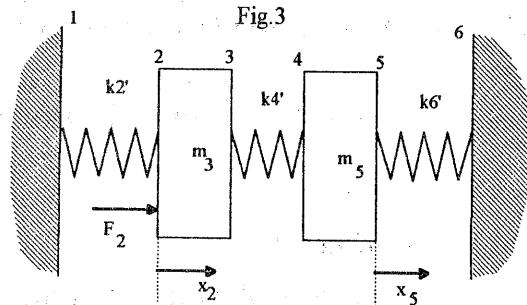
Rearranging and multiplying  $\dot{x}_5$  by  $j\omega$  to convert from velocity to acceleration

The transfer inertance

$$\ddot{x}_5 / F_2 = [j\omega T_{23} T_{34} e^{-jk_5 l_5} (1 + R_5) (Z_{in2} + z_3)] / [Z_{in5} (Z_{in2} + Z_{in-2}) \pi d^2 / 2]$$

### 2.2 Lumped Parameter Model

Figure 3 shows a schematic of the lumped parameter model of the testrig shown in Figure 1. The boundary and layer numbers have been kept the same as the wave model for ease of comparison.



$k'_2$  = complex 'spring' stiffness of air layer 2 =  $k_2(1 + j \tan \delta_2)$  where  $k_2 = \rho_2 c_2^2 \pi d^2 / 4 l_2$   
and  $\tan \delta_2$  = loss factor of air layer

$k'_4$  = complex spring stiffness sample layer 4 =  $k_4(1 + j \tan \delta_4)$  where  $k_4 = \rho_4 c_4^2 \pi d^2 / 4 l_4$   
and  $\tan \delta_4$  = loss factor of sample

and similarly  $k'_6$  = complex stiffness of air layer 6

Summing the forces at boundary 2 gives

$$F_2 - m_3 \ddot{x}_2 - k'_2 x_2 - k'_4 (x_2 - x_5) = 0$$

Summing forces at boundary 5 gives

$$k'_4 (x_2 - x_5) - m_5 \ddot{x}_5 - k'_6 x_5 = 0$$

Replacing  $\ddot{x}_2$  by  $-\omega^2 x_2$  and  $\ddot{x}_5$  by  $-\omega^2 x_5$  gives

$$F_2 + m_3 \omega^2 x_2 - k'_2 x_2 - k'_4 x_2 + k'_4 x_5 = 0$$

and  $k'_4 x_2 - k'_4 x_5 + m_5 \omega^2 x_5 - k'_6 x_5 = 0$

Rearranging these into matrix notation gives

$$\begin{bmatrix} x_2 \\ x_5 \end{bmatrix} = \text{inv} \left[ \begin{bmatrix} m_3 & 0 \\ 0 & m_5 \end{bmatrix} \omega^2 + \begin{bmatrix} -(k'_2 + k'_4) & k'_4 \\ k'_4 & -(k'_4 + k'_6) \end{bmatrix} \right] \times \begin{bmatrix} -F_2 \\ 0 \end{bmatrix}$$

## COMPLEX IMPEDANCE MEASUREMENTS OF ACOUSTICAL TREATMENTS

Similarly the stiffness matrix can be determined from the response matrix. However, in order for the resulting matrix expression to be capable of inversion the number of unknowns must not exceed two.

Now  $x_2, x_5, F_2, \omega, m_3$  and  $m_5$  are measured leaving  $k'_2, k'_4$  and  $k'_6$  as the unknowns.

Since the air spring actuators can be exactly the same design and as they will be charged to the same pressure it is reasonable to assume that  $k'_6 = k'_2$

Therefore the stiffness matrix can be expressed

$$\begin{bmatrix} k'_2 \\ k'_4 \end{bmatrix} = \text{inv} \begin{bmatrix} x_2 & (x_2 - x_5) \\ x_5 & -(x_2 - x_5) \end{bmatrix} \times \left[ \begin{bmatrix} m_3 x_2 \\ m_5 x_5 \end{bmatrix} \omega^2 + \begin{bmatrix} F_2 \\ 0 \end{bmatrix} \right]$$

If the real part of  $k'_4 = \text{Re}\{k'_4\}$  and the imaginary part of  $k'_4 = \text{Im}\{k'_4\}$

Then the loss factor of the sample as a function of frequency

$$\tan \delta_4(\omega) = \text{Im}\{k'_4(\omega)\} \div \text{Re}\{k'_4(\omega)\}$$

and the real phase speed of the sample as a function of frequency

$$c_4(\omega) = \sqrt{4l_4 \text{Re}\{k'_4(\omega)\} / \rho_4 \pi d^2}$$

### 3. RESULTS

#### 3.1 Theoretical Results

Figure 4. Predicted frequency response of a typical spring-like sample

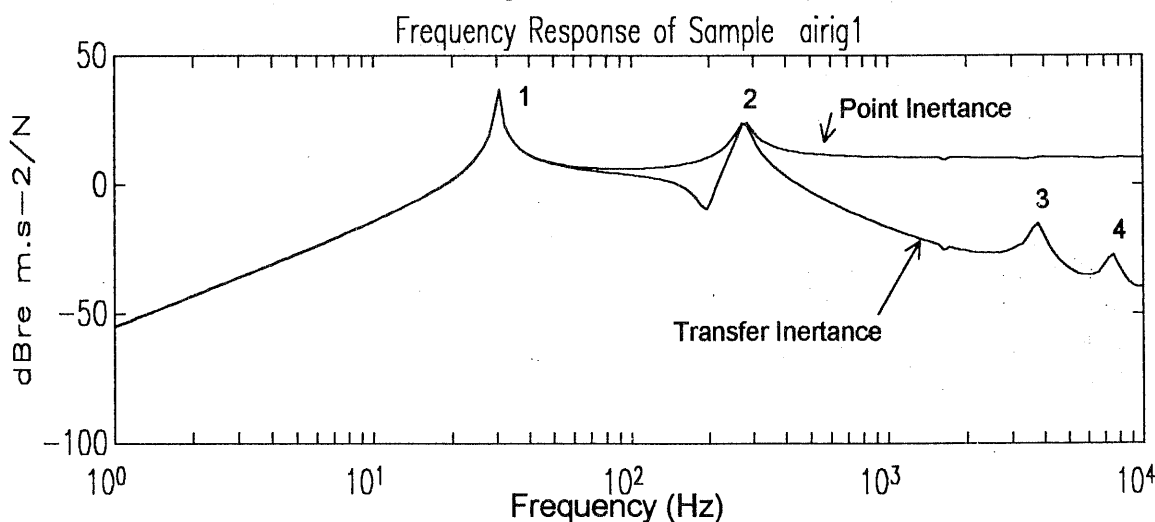
Phase Speed = 150 m/s, Loss Factor = 0.1, Thickness = 20mm, Dia = 100mm

Density = 50 kg/m<sup>3</sup>

Aluminium Terminating Masses 100mm dia, 14mm Thick

Air actuators 100mm dia, 100mm long

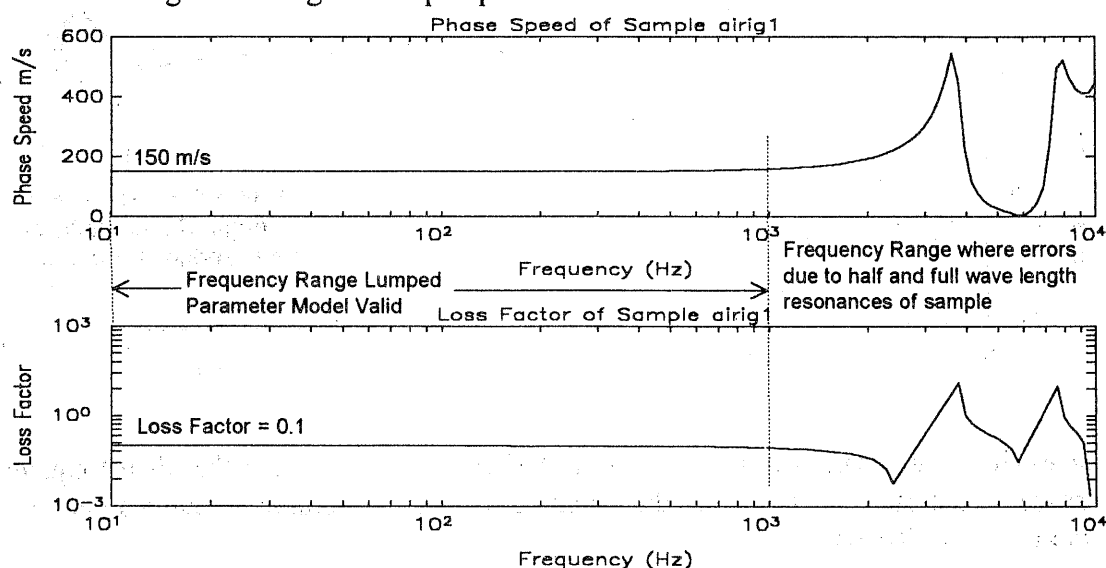
Hydrostatic Pressure = 1 bar



## COMPLEX IMPEDANCE MEASUREMENTS OF ACOUSTICAL TREATMENTS

Figure 4 overleaf shows the predicted frequency response of a typical spring-like sample using the multilayer one dimensional wave model. The resonant peak 1 is the 'rigid body' resonance of the terminating mass-sample-mass on the air spring actuators. Resonant peak 2 is the resonance of the terminating masses on the sample and experimental results have shown that the frequency at which this resonance occurs is important because it is in this frequency range that the most accurate sample phase speed and loss factor estimates are made. Resonant peaks 3 and 4 are the

Figure 5. Phase speed and loss factor from inversion of frequency responses shown in Figure 4 using the lumped parameter model



half-wave and full-wave length resonances of the sample respectively.

Figure 5 shows the inversion results of the frequency response for the spring-like sample shown in Figure 4 using the lumped parameter model for the inversion. The correct values for the phase speed and loss factor are 150m/s and 0.1. It can be seen that, in this example, the inversion has been accurate up to approximately 1kHz, above which the sample half and full wave length resonance effects become significant. The half-wave sample resonance represents the upper frequency limit where the two degree of freedom lumped parameter model can be successfully used for inversion. The frequency  $f$  at which this occurs is a function of sample phase speed  $c_{\text{sample}}$  and its thickness  $t$  i.e.  $f = c_{\text{sample}}/2t$ .

To demonstrate the effects of static load upon the frequency response of the spring-like sample used in the previous example, Figure 6 overleaf shows the predicted frequency response for a simulated hydrostatic pressure load equivalent to 100m of sea water. It has been assumed that the phase speed and loss factor of the sample have remained the same i.e. 150m/s and 0.1 respectively. For the purposes of this example the thickness of the sample has been assumed to reduce in accordance with Boyle's law i.e. from 20mm to 2mm, which results in a density of 500 kg/m<sup>3</sup>.

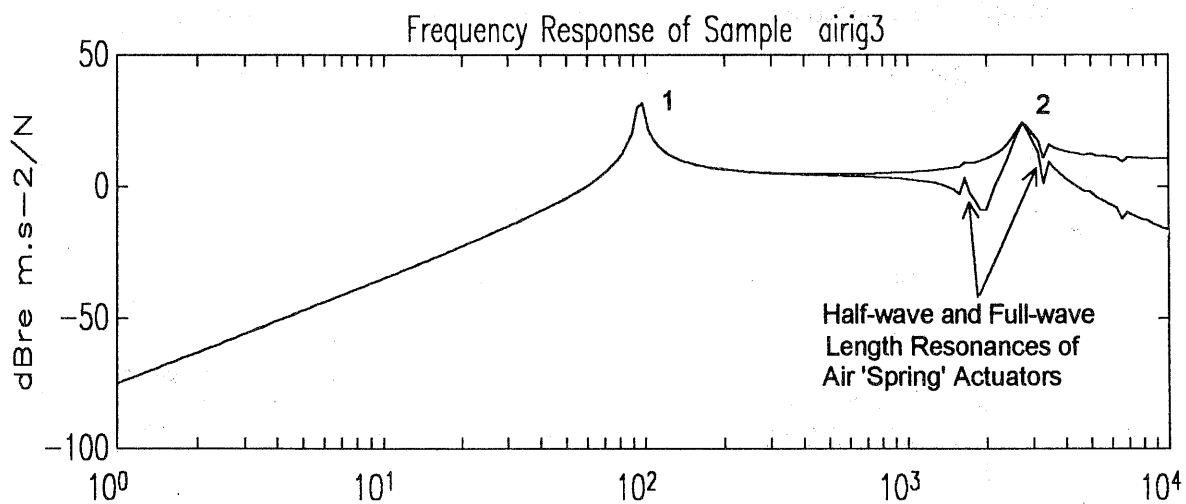
# COMPLEX IMPEDANCE MEASUREMENTS OF ACOUSTICAL TREATMENTS

Figure 6. Predicted frequency response of a typical spring-like sample under a simulated hydrostatic pressure load equivalent to a depth of 100m sea water

Phase Speed =150 m/s, Loss Factor=0.1, Thickness=2mm, Dia =100mm

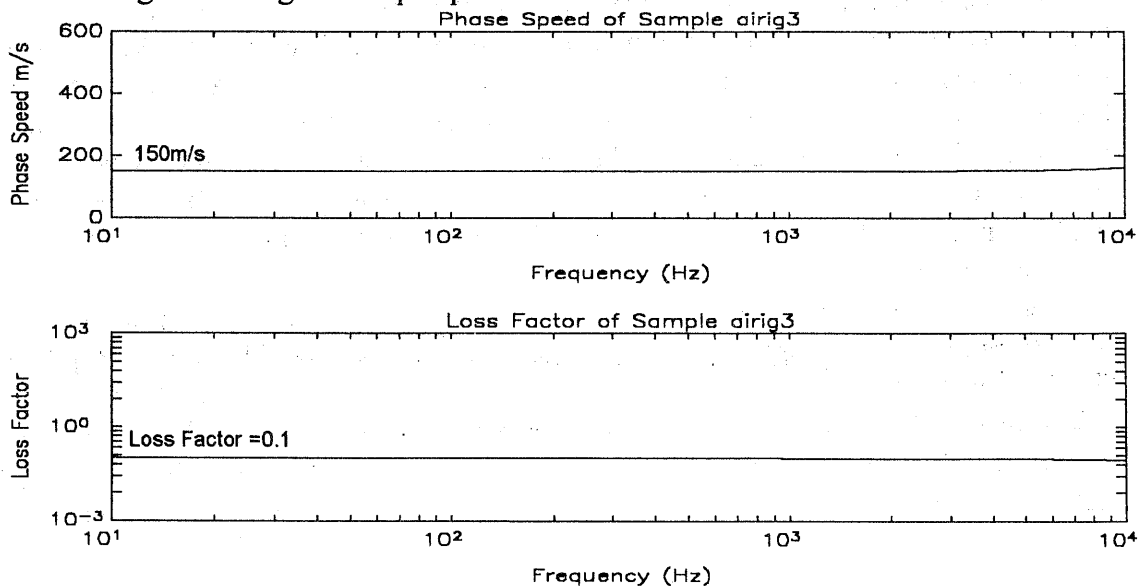
Density =500 kg/m<sup>3</sup>

Aluminium Terminating Masses 100mm dia, 14mm Thick



The modes of resonant peaks 1 and 2 are as before but it can be seen that their frequencies have increased significantly as a result of the sample and air spring actuators having an increased compressional stiffness.

Figure 7. Phase speed and loss factor from inversion of frequency responses shown in Figure 6 using the lumped parameter model



## COMPLEX IMPEDANCE MEASUREMENTS OF ACOUSTICAL TREATMENTS

This is due to their increase in density as a result of the applied load (the phase speed of air is independent of pressure for moderate pressures and is a constant 330m/s at 2° C). The increased stiffness of the air spring actuators has also resulted in a reduced inertance in the frequency range below resonant peak 1 and their half-wave and full-wave length resonances are now becoming apparent at 1650 Hz and 3300 Hz respectively. It should be noted however that the sample length resonances are now well out of the frequency range of interest as a result of the sample being significantly reduced in length due to the applied load.

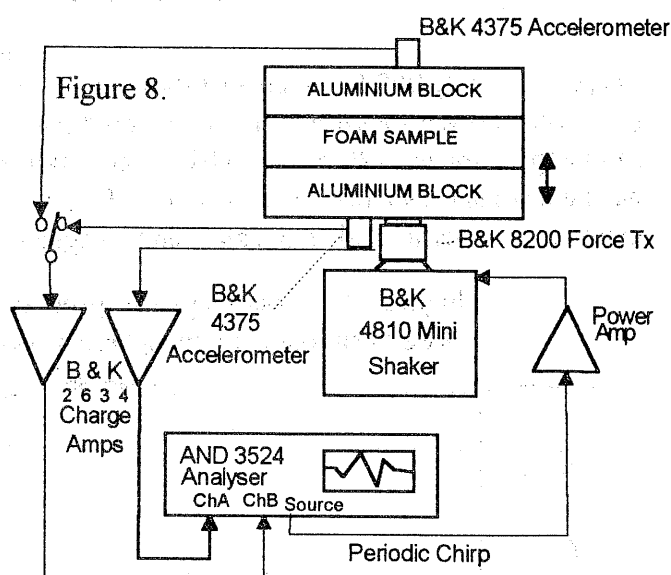
The inversion results using the lumped parameter model are shown in Figure 7 on the previous page. It can be seen that despite the significant change in compressional stiffness of both the sample and the air spring actuators, the inversion has been successful in determining the correct phase speed and loss factor of the sample up to 10kHz. Somewhat surprising is the insignificant effect the length resonances of the air 'spring' actuators have had upon the result despite their influence being apparent in the frequency response predictions.

### 3.2 Experimental Results

At the time of writing the air 'spring' actuators await manufacture and experimental measurements of samples under load have therefore not yet been carried out. However, Figure 8 is a schematic diagram of the experimental set up used for the phase speed and loss factor measurement of a 20mm thick, 100mm diameter low density 'closed cell' foam at atmospheric pressure. The sample was sandwiched between two circular 14mm thick, 100 mm diameter aluminium plates using self adhesive tape. These circular plates represent the two terminating masses mentioned previously and it should be noted that the thickness and material selection for these was carefully chosen in order that in the frequency range of interest 10Hz-1kHz, they may be considered as being 'mass-like'. It was confirmed experimentally that the first resonant frequency of the circular plates was 6.3kHz which corresponded to the first flexural bending mode. This is considered to be sufficiently above the highest frequency of interest, 1kHz, for the motion at 1kHz to be sufficiently plane.

Figure 9 overleaf shows the measured point and transfer inertance frequency response. It will be noted that the response is typical of a single degree of freedom system with a resonant frequency

FREQUENCY RESPONSE MEASUREMENT  
CLOSED CELL FOAM RA15 50kg/m<sup>3</sup>



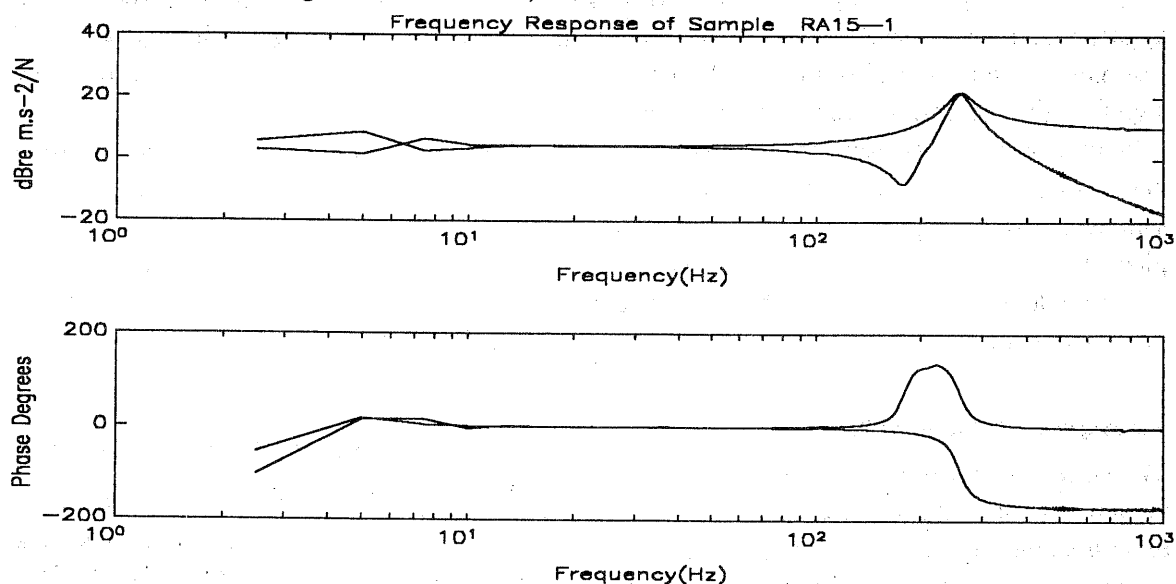


## COMPLEX IMPEDANCE MEASUREMENTS OF ACOUSTICAL TREATMENTS

Figure 9. Point and transfer inertance frequency response measurements of a low density spring-like closed cell foam at atmospheric pressure

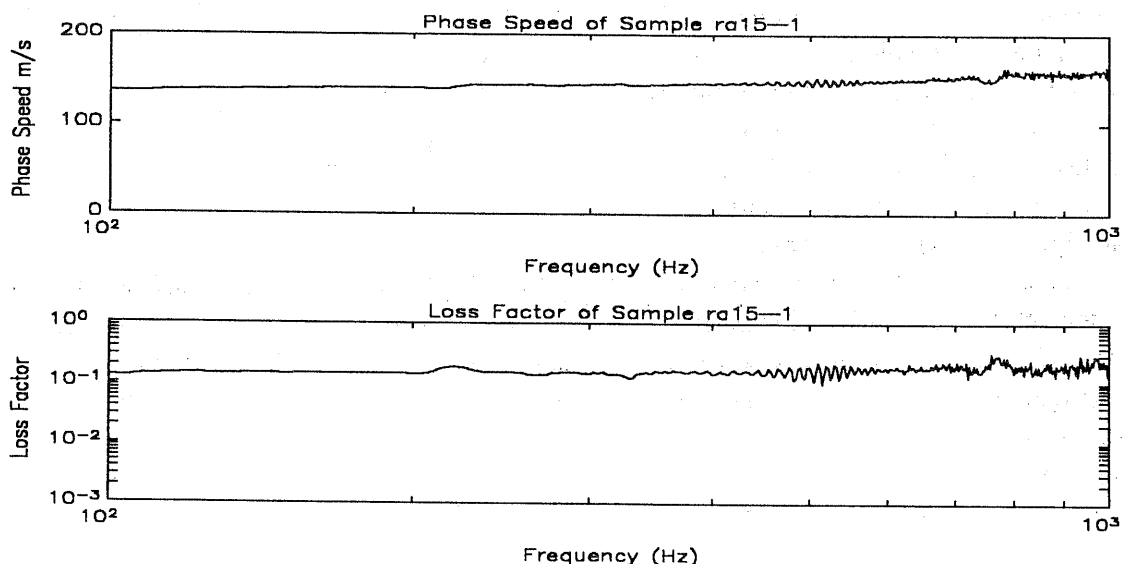
Sample Thickness=20mm, Dia =100mm Density =50 kg/m<sup>3</sup>

Aluminium Terminating Masses 100mm dia, 14mm Thick



of approximately 260 Hz. Figure 10 shows the inversion results of the measured frequency responses shown in Figure 9. It will be noted that the indicated phase speed increases steadily from approximately 140m/s at 100Hz to approximately 160m/s at 1kHz with the loss factor having a constant value of approximately 0.1. The small fluctuations are attributable to extraneous experimental errors and can be neglected. Confirmation of the accuracy of the phase

Figure 10. Measured phase speed and loss factor of a Low density spring-like closed cell foam at atmospheric pressure



## COMPLEX IMPEDANCE MEASUREMENTS OF ACOUSTICAL TREATMENTS

speed estimate was obtained with a higher frequency measurement where the sample half wave resonant frequency was observed to be 4.1kHz which corresponds to 165 m/s for a sample thickness of 20mm. The loss factor estimate of 0.1 has not been confirmed but is considered to be probably reliable for the material from which the sample is manufactured. Results below 100Hz are not presented. It has already been mentioned that the most accurate measurements are obtained in the frequency range around the resonant frequency of the terminating masses on the sample. With the terminating masses used for this measurement giving a resonant frequency of approximately 260 Hz it is considered that larger masses were needed for accurate phase speed estimates to be obtained down to 10Hz.

### 4. CONCLUSIONS

The results so far indicate that the proposed technique has the potential at least to be considered a possible method for determining the acoustic characteristics of underwater acoustical treatments. It has been demonstrated theoretically that a lumped parameter model can be successfully used to 'invert' measured sample frequency responses to determine the complex phase speed of spring-like samples under simulated hydrostatic pressure loads. Bearing in mind the acoustical characteristics of typical spring-like treatments used in underwater applications the technique should be useful over the frequency range 10Hz-1 kHz. The principle of the technique has been confirmed experimentally using a low density closed cell foam although this was done at atmospheric pressure in the absence of a mechanical arrangement for the simulation of hydrostatic pressure loads. Before the technique can be considered as a possible alternative to the water loaded impedance tube further research is obviously necessary. It is planned that this will include the experimental evaluation of air spring actuators to simulate hydrostatic pressure loads and a wave model 'inversion' to measure the complex phase speed of a wide range of non spring-like treatments.

### 5. REFERENCES

- [1] D.M.Norris Wun-Chun Young 'Complex modulus measurement by longitudinal vibration testing' 1970 Exp.Mech. 10
- [2] T.Pritz 'Transfer function method for investigating the complex modulus of acoustic materials:spring-like specimen' Jour.Sound & Vib.1980 72
- [3] S.O.Oyadiji G.R.Tomlinson 'Determination of the complex moduli of viscoelastic structural elements by resonance and non-resonance methods' Jour.Sound & Vib. 1985 101(3)
- [4] W.M.Madigosky G.F.Lee 'Improved resonance technique for materials characterisation' J.Acoust.Soc.Am. 1983 73(4)
- [5] J.L.Buchanan 'Numerical solution for the dynamic moduli of a viscoelastic bar' 1987 J.Acost.Soc.Am 1987 81(6)
- [6] Brekovskikh 'Waves in layered media'
- [7] L.E.Kinsler A.R.Frey 'Fundamentals of Acoustics' J.Wiley & Sons 1982